

Epitaxial Electrodeposition of Copper(I) Oxide on Single-Crystal Copper

Julie K. Barton, Alexey A. Vertegel, Eric W. Bohannon, and Jay A. Switzer*

Department of Chemistry and Graduate Center for Materials Research, University of Missouri–Rolla, Rolla, Missouri 65409-1170

Received September 5, 2000. Revised Manuscript Received December 6, 2000

Epitaxial thin films of copper(I) oxide ($Pn3m$, $a = 0.427$ nm) were electrodeposited onto [110]-, [111]-, and [100]-oriented single-crystal copper ($Fm3m$, $a = 0.3615$ nm) by reduction of copper(II) lactate in solution. Cu_2O films grown on Cu(110) and Cu(111) exhibited both an out-of- and in-plane orientation following that of the substrate as measured by 2θ and azimuthal X-ray scans, up to a thickness of $0.8 \mu\text{m}$. X-ray diffraction studies showed that Cu_2O films deposited onto Cu(100) grow initially with a near-[111] orientation up to a critical thickness, beyond which film growth is primarily in the [100] direction. The films were found to be both in- and out-of-plane oriented throughout, as measured by azimuthal X-ray scans. In situ 2θ X-ray measurements showed a critical thickness for growth in the [100] direction of about 360 nm. As determined from scanning electron microscopy images, the Cu_2O films deposited onto Cu(100) grew with triangular facets consistent with the [111] orientation prior to the critical thickness, and then as pyramidal islands over the initial triangular layers above this thickness. A proposed interface model of $\text{Cu}_2\text{O}(111)$ over Cu(100) yields a low mismatch and a high number of atomic contact points per unit area, offering a possible explanation for the initial [111]-oriented deposition.

Introduction

Electrodeposition is a simple and inexpensive technique for preparing epitaxial films. We have recently electrodeposited epitaxial thin films of $\delta\text{-Bi}_2\text{O}_3$, Cu_2O , PbS, Ti_2O_3 , Fe_3O_4 , and a $\text{Cu}_2\text{O}/\text{PbS}$ heterojunction onto single-crystal Au.^{1–7} However, little work has been done with epitaxial electrodeposition onto substrates other than Au. In the present work, it is shown that this technique may be extended to the deposition of epitaxial thin films of Cu_2O onto single-crystal Cu.

Cu_2O is a p -type semiconductor that has been electrodeposited previously on a variety of substrates.^{8–11} In previous studies of the electrodeposition of Cu_2O films, we have demonstrated that the out-of-plane orientation of a film deposited on a polycrystalline

substrate is dependent on the solution pH.¹² In addition, scanning electron microscopy (SEM) images revealed that these films grow with a faceted microstructure corresponding to the out-of-plane orientation of the film, yielding four-sided pyramids or triangular structures for [100]- and [111]-oriented films, respectively.¹² Lee et al. deposited Cu_2O onto Pt from a weakly acidic solution and reported a film with a [111] out-of-plane orientation.¹³ In both experiments, geometric facets grew with no particular orientation within the plane of the film.

In other studies, we have shown that the deposition current for the Cu_2O is limited by a Schottky-like barrier that forms between Cu_2O and the deposition solution.¹² We have also shown that under certain galvanostatic conditions the working electrode potential spontaneously oscillates,^{14,15} forming a Cu/ Cu_2O -layered nanostructure that shows a negative differential resistance (NDR) feature during perpendicular transport measurements.¹⁶ The $1/L^2$ dependence of the NDR feature on the Cu_2O layer thickness suggests quantum confinement of carriers in the nanoscale Cu_2O .¹⁷ Although these layered nanostructures have, at present, only been deposited on polycrystalline substrates, it

* E-mail: jswitzer@umr.edu.

(1) Switzer, J. A.; Shumsky, M. G.; Bohannon, E. W. *Science* **1999**, *284*, 293.

(2) Bohannon, E. W.; Jaynes, C. C.; Shumsky, M. G.; Barton, J. K.; Switzer, J. A. *Solid State Ionics* **2000**, *131*, 97.

(3) Vertegel, A. A.; Shumsky, M. G.; Switzer, J. A. *Angew. Chem., Int. Ed. Engl.* **1999**, *38*, 3169.

(4) Bohannon, E. W.; Shumsky, M. G.; Switzer, J. A. *Chem. Mater.* **1999**, *11*, 2289.

(5) Vertegel, A. A.; Shumsky, M. G.; Switzer, J. A. *Electrochim. Acta* **2000**, *45*, 3233.

(6) Nikiforov, M. P.; Vertegel, A. A.; Switzer, J. A. *Adv. Mater.* **2000**, *12*, 1351.

(7) Vertegel, A. A.; Shumsky, M. G.; Switzer, J. A. *Chem. Mater.* **2000**, *12*, 596.

(8) Mukhopadhyay, A. K.; Chakraborty, A. K.; Chatterjee, A. P.; Lahiri, S. K. *Thin Solid Films* **1992**, *209*, 92.

(9) Chatterjee, A. P.; Mukhopadhyay, A. K.; Chakraborty, A. K.; Sasmal, R. N.; Lahiri, S. K. *Mater. Lett.* **1991**, *11*, 358.

(10) Rakhshani, A. E.; Varghese, J. *Thin Solid Films* **1988**, *157*, 87.

(11) Tench, D.; Warren, L. F. *J. Electrochem. Soc.* **1983**, *130*, 869.

(12) Golden, T. D.; Shumsky, M. G.; Zhou, Y.; Vanderwerf, R. A.; Van Leeuwen, R. A.; Switzer, J. A. *Chem. Mater.* **1996**, *8*, 2499.

(13) Lee, J.; Tak, Y. *Electrochem. Solid-State Lett.* **1999**, *2*, 559.

(14) Bohannon, E. W.; Huang, L.-Y.; Miller, F. S.; Shumsky, M. G.; Switzer, J. A. *Langmuir* **1999**, *15*, 813.

(15) Switzer, J. A.; Hung, C.-J.; Huang, L.-Y.; Miller, F. S.; Zhou, Y.; Raub, E. R.; Shumsky, M. G.; Bohannon, E. W. *J. Mater. Res.* **1998**, *13*, 909.

(16) Switzer, J. A.; Hung, C.-J.; Huang, L.-Y.; Switzer, E. R.; Kammler, D. R.; Golden, T. D.; Bohannon, E. W. *J. Am. Chem. Soc.* **1998**, *120*, 3530.

(17) Switzer, J. A.; Maune, B. M.; Raub, E. R.; Bohannon, E. W. *J. Phys. Chem. B* **1999**, *103*, 395.

would be desirable for device applications to deposit these structures as epitaxial films on single-crystal substrates. A study of the deposition and growth behavior of Cu_2O on Cu single-crystal substrates may prove a useful starting point to developing epitaxial Cu/ Cu_2O -layered nanostructures.

A significant amount of work has been done concerning oxide growth in the monolayer range on copper substrates. Gewirth et al. have made in situ observations of oxide growth on Cu(111) in both aqueous and native environments, and found epitaxial $\text{Cu}_2\text{O}(111)$ to form in both cases.¹⁸ Gewirth et al. have also studied oxygen adsorption on a Cu(100) surface and reported a $(\sqrt{2} \times \sqrt{2})R45^\circ$ adlattice.¹⁹ Ikemaya et al. studied aqueous oxide formation on Cu(100) and Cu(111) substrates, with results agreeing with those reported by Gewirth et al. They suggested coincidence lattices of $(6 \times 6)\text{Cu}_2\text{O}(111)/(7 \times 7)\text{Cu}(111)$ and $(6 \times 6)\text{Cu}_2\text{O}(100)-[001]/(5 \times 5)\text{Cu}(100)[011]$, respectively.²⁰

Little research has been done on the electrodeposition of bulk Cu_2O films on copper substrates, and research on the electrodeposition of epitaxial Cu_2O on Cu grown to thicknesses in the micron range has yet to be reported. Santra et al. electrodeposited Cu_2O films onto polycrystalline copper from a copper lactate solution and studied the microstructural effects of solution pH and film annealing temperature, reporting an optimum solution pH of 9.2–9.3.²¹ In the present work, we extend our study of epitaxial electrodeposited films to that of Cu_2O on low-index Cu single-crystal substrates. Films grown to a maximum thickness of 0.8 μm on Cu(110) and (111) exhibited orientations of [110] and [111], respectively, whereas films deposited on Cu(100) grew with an initial orientation of [111], transforming after a certain thickness into a [100] orientation. All films exhibit epitaxial growth with respect to the Cu substrate.

Experimental Section

The deposition solution was prepared by adding 450 mL of 5 M NaOH to 90 g of Cu(II) sulfate pentahydrate and 150 mL of 85+% lactic acid. The solution was adjusted to pH 9.0 with further additions of aqueous 5 M NaOH. Water was HPLC-grade (Aldrich), and all other chemicals were reagent-grade (Aldrich). Working electrodes consisted of 1 cm diameter Cu(110), Cu(111), and Cu(100) single crystals purchased from the Monocrystals company. A copper wire fitted around the edge of the crystals served as the electrical contact during deposition. A large area copper wire was used as the counter electrode. In all experiments, a constant cathodic current density of 0.03 mA/cm^2 was applied to the working electrodes with an EG&G Princeton Applied Research model 273A potentiostat/galvanostat. The deposition rate was 0.037 nm/s. Deposition times ranging from about 5000 to 80 000 seconds, yielding films in the thickness range of 0.2–3.0 μm .

Prior to deposition, the Cu electrodes were electropolished in a 67 vol % orthophosphoric acid aqueous solution at a potential of 1.45 V versus SCE. Immediately before deposition, the electrodes were treated with a drop of 0.1 M HClO_4 to remove any native oxide present. With the exception of the in

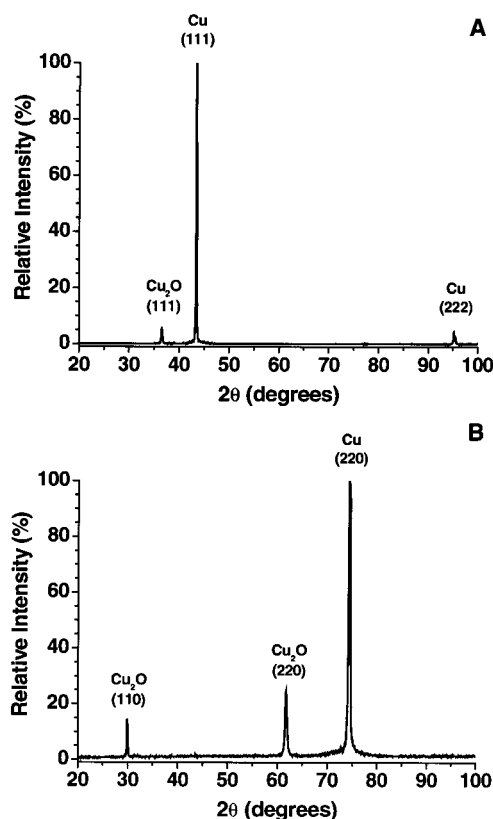


Figure 1. 2θ X-ray patterns of 0.7 μm thick Cu_2O films deposited on (A) Cu(111) and (B) Cu(110). Both films followed the orientation of the Cu substrates.

situ XRD experiments, the deposition solution was kept at a constant temperature of 30 $^\circ\text{C}$ with a Fisher model 9100 circulator, and constant stirring was applied. X-ray diffraction (XRD) experiments were performed with a Scintag 2000 diffractometer using Cu $K\alpha$ radiation. Azimuthal and tilt scans were obtained through the attachment of a texture goniometer accessory to the Scintag 2000.

Due to the limiting conditions of the in situ XRD set up, deposition for these experiments was performed at approximately 25 $^\circ\text{C}$. In situ measurements of films grown on Cu(100) were made with the above-described potentiostat/galvanostat and Scintag instruments, again with a large area copper wire functioning as the counter electrode. The deposition solution was approximately 0.5 mm in height above the substrate, so as to minimize the absorption of X-rays by the copper lactate solution. The small volume of liquid required reconstitution every 30 min. Approximately every 10 min, 2θ scans were run, from $2\theta = 34$ – 51.5° . Micrographs of the deposited films were obtained with a Hitachi model S4700 cold-field emission scanning electron microscope.

Results and Discussion

A. Deposition of Cu_2O on Cu(111) and Cu(110).

Parts A and B of Figure 1 show 2θ X-ray diffraction patterns for films grown on Cu(111) and (110), respectively. Only those Cu_2O peaks corresponding to the orientation of the substrate are observed, indicating a strong out-of-plane orientation for both films. The patterns in Figure 1 are of films grown to a thickness of 0.7 μm ; however, 2θ scans of films over a thickness range of 0.35–0.8 μm yielded the same results.

Evidence for in-plane texture was obtained from pole figures for all films. The Bragg (θ), tilt (γ), azimuthal (ϕ), and rocking (ω) angles used in the X-ray measurements are shown in Figure 2. In generating an azi-

(18) Chu, Y. S.; Robinson, I. K.; Gewirth, A. A. *J. Chem. Phys.* **1998**, *110*, 5952.

(19) Cruickshank, J. R.; Sneddon, D. D.; Gewirth, A. A. *Surf. Sci.* **1993**, *281*, L308.

(20) Ikemaya, N.; Kubo, T.; Hara, S. *Surf. Sci.* **1995**, *323*, 81.

(21) Santra, K.; Chatterjee, S. P.; Gupta, S. *Sol. Energy Mater.* **1999**, *57*, 345.

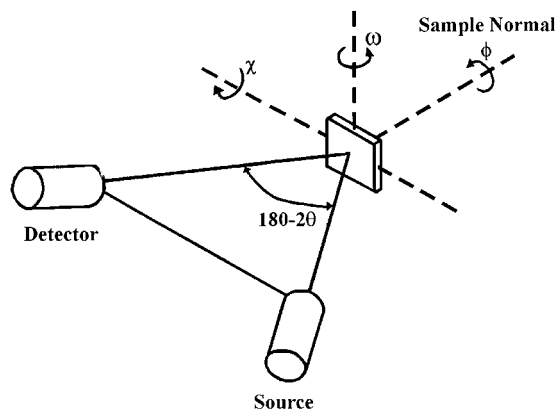


Figure 2. Schematic of the experimental setup used to determine the in- and out-of-plane orientation of epitaxial films by X-ray diffraction. The out-of-plane orientation is determined in the Bragg–Brentano configuration by standard θ – θ scans. The out-of-plane mosaicity is determined by rocking the sample about the ω -axis. Rotating the sample 360° about the ϕ -axis results in a two-dimensional azimuthal scan. Constructing azimuthal scans for a series of tilt angles, χ , results in a three-dimensional pole figure, in which the epitaxy of the film has been determined for all crystallographic planes of the substrate.

muthal pattern of an $[hkl]$ -oriented film, the X-ray source-detector system is set to a 2θ value corresponding to some other plane ($h'k'l$). The sample is then tilted about the χ -axis until the ($h'k'l$) planes are brought into the Bragg condition. The angle of tilting, χ , corresponds to the angle between the (hkl) and ($h'k'l$) planes. Rotation of the sample along the perpendicular ϕ -axis results in an azimuthal scan. A series of these azimuthal scans run over a range of tilt angles results in a three-dimensional pole figure. The pole figure of a perfectly epitaxial film should yield zero intensity at all values of χ other than that corresponding to the angle between the (hkl) and ($h'k'l$) planes.

The values of 2θ used here were experimentally determined as the angle of maximum diffracted intensity for the reflection of interest. For all pole figures, azimuthal scans were run at every 1.0° tilt as the sample was tilted from $\chi = 0$ – 80° . In generating the (220) pole figure for the [111]-oriented Cu_2O film, the X-ray detector was first set to a 2θ value of 61.35° , corresponding to the (220) Cu_2O peak. A value of $2\theta = 36.57^\circ$ was chosen for the (111) pole figure of the (110)-oriented film, corresponding to the (111) Cu_2O peak. For both films, the theoretical tilt angle for maximum intensity is $\chi = 35.3^\circ$, corresponding to the angle between the (110) and (111) planes.

The pole figures for the (111) and (100) Cu_2O films are shown in contour form in parts A and B of Figure 3, respectively. Figure 3 shows an apparent 6-fold symmetry with a maximum intensity at $\chi = 36.8^\circ$, agreeing reasonably well with the theoretical tilt angle of 35.3° . The 6-fold pattern is actually two sets of 3-fold patterns, rotated 180° about an axis perpendicular to the plane of Figure 3A. This pattern suggests that although the (111) plane of the film is parallel to the (111) plane of the Cu substrate, individual crystalline grains in the film appear to have grown either aligned with, or opposite to, the in-plane direction of the substrate. This agrees with results from previous workers.¹⁸ One set of peaks is more intense than the other,

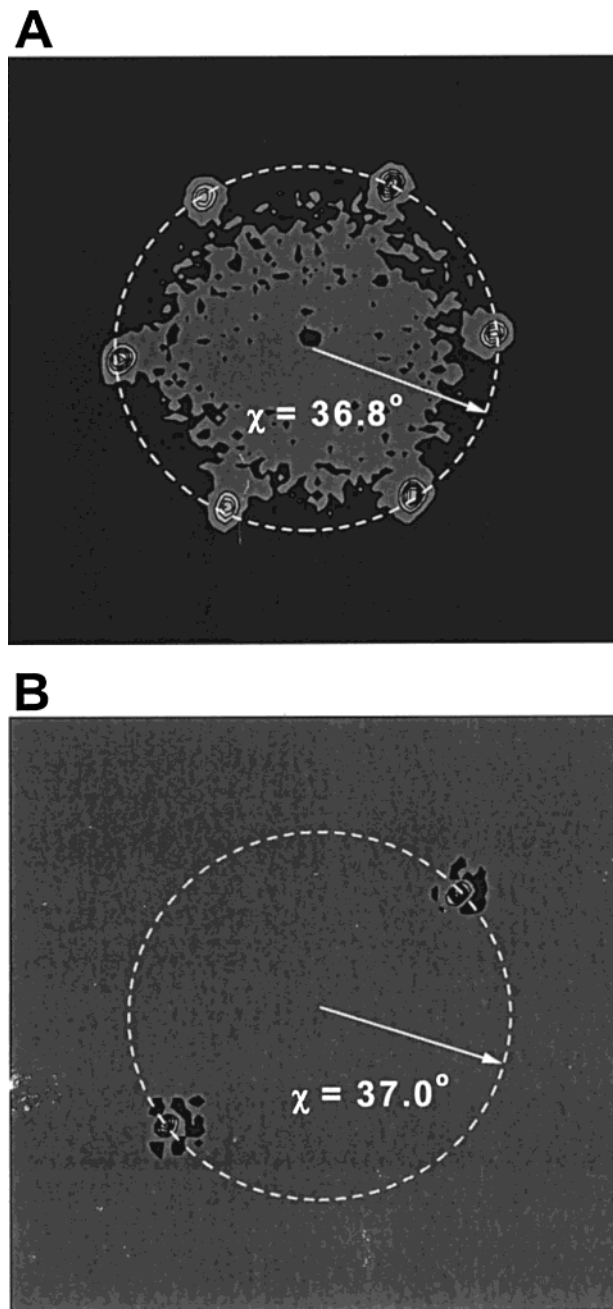


Figure 3. Contour plots of pole figures of Cu_2O films deposited on (A) Cu(111) and (B) Cu(110). Part A is a (220) pole figure with a theoretical tilt angle of $\chi = 35.3^\circ$ for the (111) plane of Cu_2O , and part B is a (111) pole figure, also with $\chi = 35.3^\circ$ theoretically. In both figures, experimentally determined tilt angles (displayed in figure) agree reasonably well with this calculated value.

and these correspond to grains that have grown aligned with the substrate. Our results show that the film is twinned, but we do not know if this twinning occurs on the substrate or if it is due to faulting during growth. Figure 3B shows a 2-fold symmetry with a maximum intensity at $\chi = 37.0^\circ$, with no observed rotation of the film relative to the Cu substrate. The peaks in Figure 3B are greater than 6000 times more intense than the background, while those in Figure 3A are only several 100–1000 times greater than the lowest background. The small increase in background intensity observed at angles of χ below 37° in Figure 3A is due to copper fluorescence.

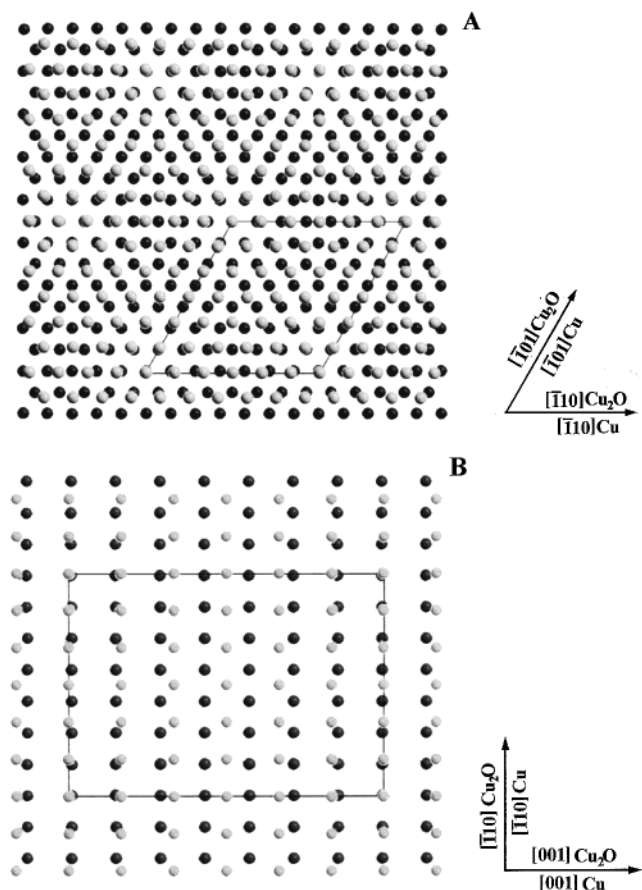


Figure 4. Models for epitaxial growth of Cu_2O on (A) $\text{Cu}(111)$ and (B) $\text{Cu}(110)$. The Cu atoms from the Cu substrate are dark, and the Cu atoms from the Cu_2O film are light. The solid lines indicate proposed coincidence unit cells. Part A shows one of the two possible epitaxial relationships, defined as $\text{Cu}_2\text{O}(111)[\bar{1}10]/\text{Cu}(111)[\bar{1}10]$. A coincidence lattice may also be formed by rotating the $\text{Cu}_2\text{O}(111)$ plane by 180° . Part B shows an epitaxial relationship of $\text{Cu}_2\text{O}(110)[001]/\text{Cu}(110)[001]$. In both cases, a coincidence lattice is formed by six Cu atoms in the Cu_2O plane to seven Cu atoms in the Cu plane and results in a mismatch of 1.22%.

Parts A and B of Figure 4 shows possible epitaxial relationships of the bulk Cu_2O films to the $\text{Cu}(111)$ and $\text{Cu}(110)$ substrates, respectively. The dark circles represent the Cu atoms of the Cu substrate, and the light circles represent the Cu atoms of Cu_2O . For Cu_2O over $\text{Cu}(111)$, the film and substrate are aligned such that the $[110]$ direction of Cu_2O is either parallel or anti-parallel to the $[110]$ of the Cu. The epitaxial relationships are thus $\text{Cu}_2\text{O}(111)[\bar{1}10]/\text{Cu}(111)[\bar{1}10]$ and $\text{Cu}_2\text{O}(111)[1\bar{1}0]/\text{Cu}(111)[\bar{1}10]$. As seen in Figure 4A, a coincidence lattice can be formed by six Cu atoms in the Cu_2O plane to every seven Cu atoms in the Cu plane. The misfit for this coincidence is 1.22%, compared with the calculated unit cell misfit of 18.1%. Figure 4B shows a $\text{Cu}_2\text{O}(110)[001]/\text{Cu}(110)[001]$ coincidence lattice, again with six Cu atoms from Cu_2O to every seven Cu atoms in the Cu plane. It should be noted that parts A and B of Figure 4 are derived from XRD measurements of the Cu_2O film, which only take into account the bulk of the material and do not say anything of the first monolayers of the Cu_2O film. These models do, however, agree with results obtained by other workers.^{18,20}

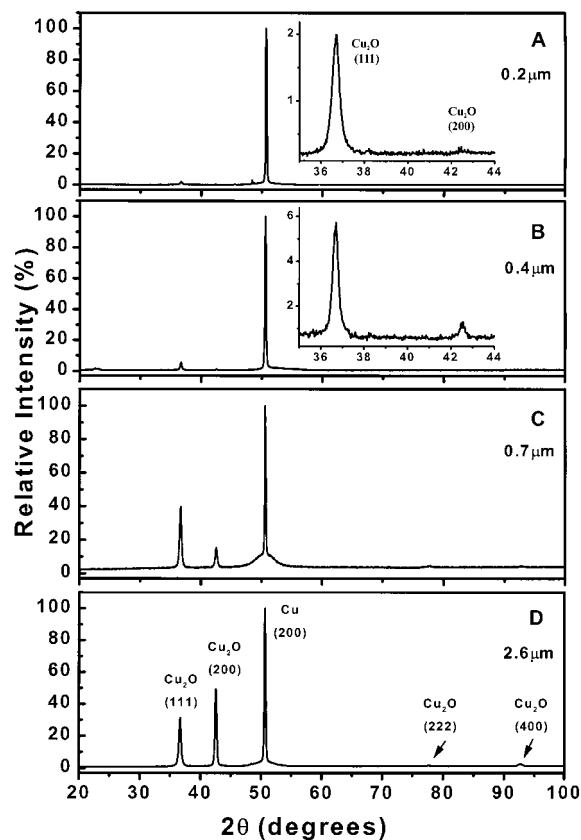


Figure 5. Ex situ 2θ X-ray patterns of four Cu_2O films deposited on $\text{Cu}(100)$, to thicknesses of (A) 0.2, (B) 0.4, (C) 0.7, and (D) $2.6 \mu\text{m}$. The patterns indicate that initial growth is in the $[111]$ direction but becomes dominated by growth in the $[100]$ direction as film thickness increases. Insets in parts A and B show the $\text{Cu}_2\text{O}(111)$ and (200) peaks at a higher magnification.

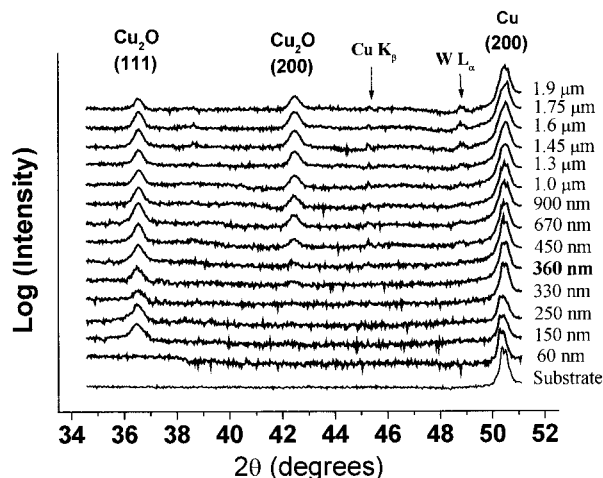


Figure 6. In situ 2θ X-ray patterns for a film grown on $\text{Cu}(100)$. Results agree with ex-situ measurements, indicating that the film grows primarily in the $[111]$ direction to a critical thickness, after which growth is primarily in the $[100]$ direction. The (200) peak for Cu_2O first appears at a thickness of 360 nm, indicating that this is approximately the critical thickness above which growth is primarily in the $[100]$ direction.

B. Deposition of Cu_2O on $\text{Cu}(100)$. Several films were deposited onto $[100]$ -oriented Cu single crystals, to thicknesses ranging from 0.2 to $2.6 \mu\text{m}$. Results of ex situ 2θ X-ray diffraction scans are shown in Figure 5. These patterns indicate that, contrary to the expected

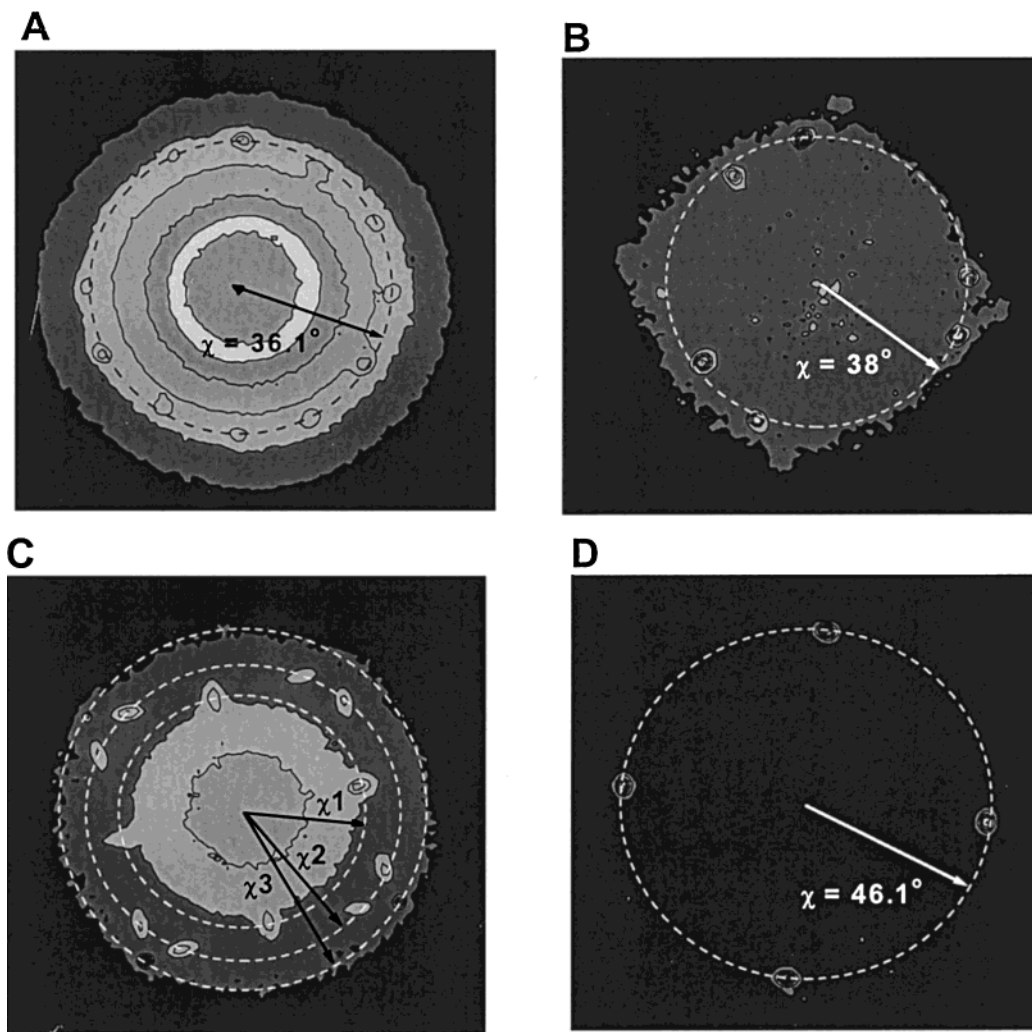


Figure 7. Contour plots of pole figure diffraction scans of Cu_2O films deposited on $\text{Cu}(100)$ to thicknesses of (A) 0.2, (B) 0.4, (C) 0.7, and (D) 2.6 μm . All figures are (220) pole figures, with a theoretical tilt angle of $\chi = 35.3^\circ$ for the (111) out-of-plane orientation of Cu_2O and $\chi = 45^\circ$ for the (100) out-of-plane orientation of Cu_2O . Parts A and D, corresponding to (111) and (100) growth, respectively, result in tilt angles (displayed in the figure) which agree reasonably well with these calculated values. Plots of films of intermediate thickness yield patterns that do not correspond to either the (111) or (100) orientations. Tilt angles in part C have values of $\chi^1 = 30.1^\circ$, $\chi^2 = 38.6^\circ$, and $\chi^3 = 46.1^\circ$.

growth of $\text{Cu}_2\text{O}(100)$, the Cu_2O film is initially dominated by growth in the [111] direction and only after some critical thickness begins to be dominated by growth in the [100] direction. At a film thickness of 0.2 μm , only the $\text{Cu}_2\text{O}(111)$ peak is clearly visible. As the film thickness increases, the (200) peak becomes visible, and its intensity increases faster than that of the (111) peak. The ratio of the (111) to (200) peak intensities decreases from 7.7 to 0.62 as the film thickness increases from 0.2 to 2.6 μm , indicating that at a thickness of 2.6 μm , the film is dominated by [100]-oriented crystals. The ratio of the intensity of the $\text{Cu}_2\text{O}(111)$ peak to the $\text{Cu}(200)$ peak remains approximately constant for thicknesses between 0.7 and 2.6 μm , whereas the $\text{Cu}_2\text{O}(200)$ peak increases by nearly 40% relative to the $\text{Cu}(200)$ peak, indicating that the growth rate in the [111] direction has decreased to a value close to zero after a thickness of $\approx 0.7 \mu\text{m}$. In situ XRD experiments were also conducted, and results agree with those obtained from the ex situ measurements. The in situ 2θ X-ray diffraction results are shown in Figure 6. The $\text{Cu}_2\text{O}(200)$ peak becomes visible at a thickness of 360 nm, showing that the thickness at which growth in the [100]

direction becomes significant is less than or equal to 360 nm.

To determine the epitaxial behavior of Cu_2O films on $\text{Cu}(100)$, the (220) pole figures shown in Figure 7 were acquired. According to the 2θ X-ray patterns, the 0.2 μm thick film should show a maximum pole figure intensity corresponding to the (111) plane, that is, at a tilt angle of $\chi = 35.3^\circ$. Similarly, the pole figure for the 2.6 μm thick film should yield a maximum intensity corresponding to the (200) plane at $\chi = 45^\circ$. Figure 7A shows 12-fold symmetry with maximum peak intensities at $\chi = 36.1^\circ$, with a deviation of about $\pm 1.9^\circ$. This symmetry is to be expected, as one can line up the triangular pattern of the $\text{Cu}_2\text{O}(111)$ planes over the square-patterned $\text{Cu}(100)$ planes four ways, thus yielding a pole figure with four sets of 3-fold patterns.

Parts B and C of Figure 7 are plots of the intermediate thicknesses of 0.4 and 0.7 μm , respectively. Figure 7B shows six distinct peaks and several indistinct peaks at tilt angles ranging from $\chi = 32.4^\circ$ – 39.0° , indicating the same 12-fold symmetry as that seen in Figure 7A. There is also an observable, though not very intense, 4-fold pattern at $\chi = 45.8^\circ$, indicating that growth in

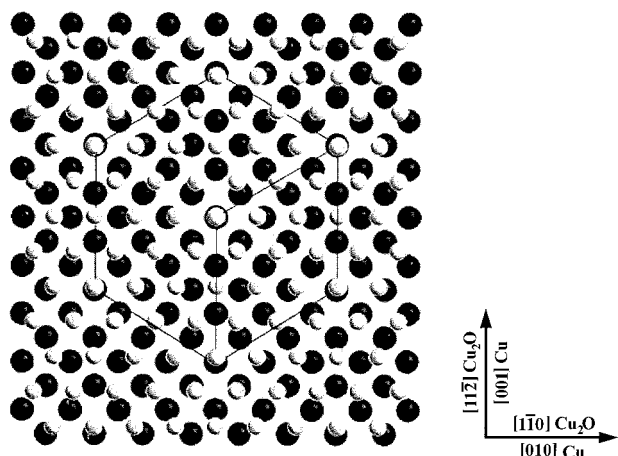


Figure 8. Proposed model for the epitaxial growth of Cu_2O -(111) on Cu (100). The Cu atoms from the Cu substrate are dark, and the Cu atoms from the Cu_2O film are light. The solid lines indicate the proposed coincidence unit cell, which is hexagonal. The epitaxial relationship of Cu_2O (111)[$11\bar{2}$]/ Cu -(100)[001] yields a mismatch of 3.57% along the Cu_2O [$11\bar{2}$]/ Cu [001] direction. This proposed model results in over twice as many contact points per square centimeter as that of Cu_2O -(100) on Cu (100).

the [100] direction has begun. Figure 7C shows what appears to be a 4-fold pattern at an average of $\chi = 30.1^\circ$, a combination of two 4-fold patterns at $\chi = 38.6^\circ$, and another 4-fold pattern at $\chi = 46.1^\circ$. These two figures indicate that at the intermediate thicknesses, a transformation from a [111] to a [100]-oriented Cu_2O film is taking place. As in Figure 3, Cu radiation caused a slight increase in background intensity at low tilt angles for Figure 7A–C, where peak intensity is low. The pole figure in Figure 7D shows 4-fold symmetry, with a maximum intensity at $\chi = 46.1^\circ$, with no rotation of the pattern relative to that of the Cu substrate, indicating that the film is primarily [100]-oriented and strongly epitaxial.

Figure 8 shows one of the four possible alignments of the Cu_2O (111) over the Cu (100). Three similar patterns can be obtained by rotating the Cu_2O (111) plane every 90° over a span of 360° . The Cu atoms of the Cu substrate are dark, and the Cu atoms of Cu_2O are light. The directions of alignment were obtained by XRD azimuthal scans, and result in a Cu_2O (111)[$11\bar{2}$]/ Cu -(100)[001] coincidence lattice. The calculated mismatch for this coincidence is 3.57% along the [$11\bar{2}$] Cu_2O direction. The number of coincident points per unit area as calculated from this model is 1.4×10^{14} points/ cm^2 . This value is roughly 2.3 times the value of 6.1×10^{13} points/ cm^2 , as obtained for the previously mentioned (6 \times 6) Cu_2O (100)[001]/(5 \times 5) Cu (100)[011] model.^{19,20} Again, this model is determined by XRD, and the orientation of the first monolayers of the film is unknown. If this model can be applied to the first monolayers of growth, then the significant increase in contact points per unit area may be a primary driving force behind these somewhat surprising results.

As mentioned in the Introduction, we have previously found that Cu_2O deposited onto polycrystalline substrates from a solution of pH 9.0 grows with a kinetically preferred [100] orientation.¹² The same result is seen on single-crystal gold substrates with orientations other than (100). Growth initially follows that of the substrate

but after a certain thickness is dominated by growth in the [100] direction.⁴ In the case of deposition onto Cu -(100), the film grows initially in the [111] direction due to the influence of the substrate as described above. However, as the film thickness increases, the kinetically preferred growth in the [100] direction begins to dominate. In addition, it does not appear that [100]-oriented crystals nucleate instantaneously on the [111]-oriented film, but rather that the growth direction of the film slowly tilts away from the [111], so that the [111] axis is no longer perpendicular to the substrate. This kind of growth has been observed in the chemical vapor deposition (CVD) of diamond films grown at higher than optimum temperatures.²² It is reported by Wild et al. that the initially deposited diamond films are (100)-oriented, but as growth continues, the texture axis of the film tilts away from the [100] direction, resulting in pole scans similar to those obtained here. Growth along near-low index directions such as the [100] or [111] can also be interpreted as growth along high Miller index directions that are tilted several degrees relative to their low-index counterparts. Clausing et al. observed such an orientation for a diamond film, reporting a (17 3 0) texture for which the (100) planes are tilted 9° from parallel to the substrate.²³

The pole figure results shown in Figure 7 may now be better understood, because as planes tilt away from parallel to the substrate, the tilt angles at which they are observed in the pole figures will also change. The angle, α , to which the (111) planes are tilted relative to the surface of the substrate can be calculated from the X-ray pole figures. In this specific case it appears that the (111) planes are tilting such that one apex of the triangular (111) plane points downward to the substrate. It can be shown that for each set of tilted (111) planes, one of the (110) planes requires a smaller degree of tilting, and two require greater tilting to enter into the Bragg condition than for the case in which the (111) planes are parallel to the substrate. The angle between the (110) and (111) planes is 35.3° , and so a pole figure for this situation will result in a 3-fold pattern for which one peak is located at $\chi < 35.3^\circ$ and two at $\chi > 35.3^\circ$. As stated above, there are four ways in which (111) planes may align above (100) planes, and so the pattern repeats itself four times, yielding a pole figure like that shown in Figure 7C. The similarity between the tilt angles observed in parts B and C of Figure 7, both of which contain (100)-oriented crystals, indicates that although growth does continue in the near-[111] direction beyond a film thickness of $0.4 \mu\text{m}$, the increase in tilting away from the [111] direction is very slight. It therefore appears that the angles observed for the $0.7 \mu\text{m}$ film represent the critical angles to which the (111) planes tilt occur before growth begins in the [100] direction. A value of $\alpha = 5.47^\circ$ has been calculated from the pattern observed in Figure 7C, which yields a calculated $\chi^1 = 29.8^\circ$ and $\chi^2 = 38.3^\circ$. These values agree well with the experimentally determined (pole figure)

(22) Wild, C.; Koidl, P.; Mueller-Sebert, W.; Walcher, H.; Kohl, R.; Herres, N.; Locher, R.; Samlenski, R.; Brenn, R. *Diamond Relat. Mater.* **1993**, *2*, 158.

(23) Clausing, R. E.; Heatherly, L.; Specht, E. D. *Diamond and Diamond-like Films and Coatings*. In *NATO Advanced Studies Institute Series, Serial B(266)*; Clausing, R. E., Horton, L. L., Angus, J. C., Koidl, P., Eds.; Plenum: New York, 1992; p 611.

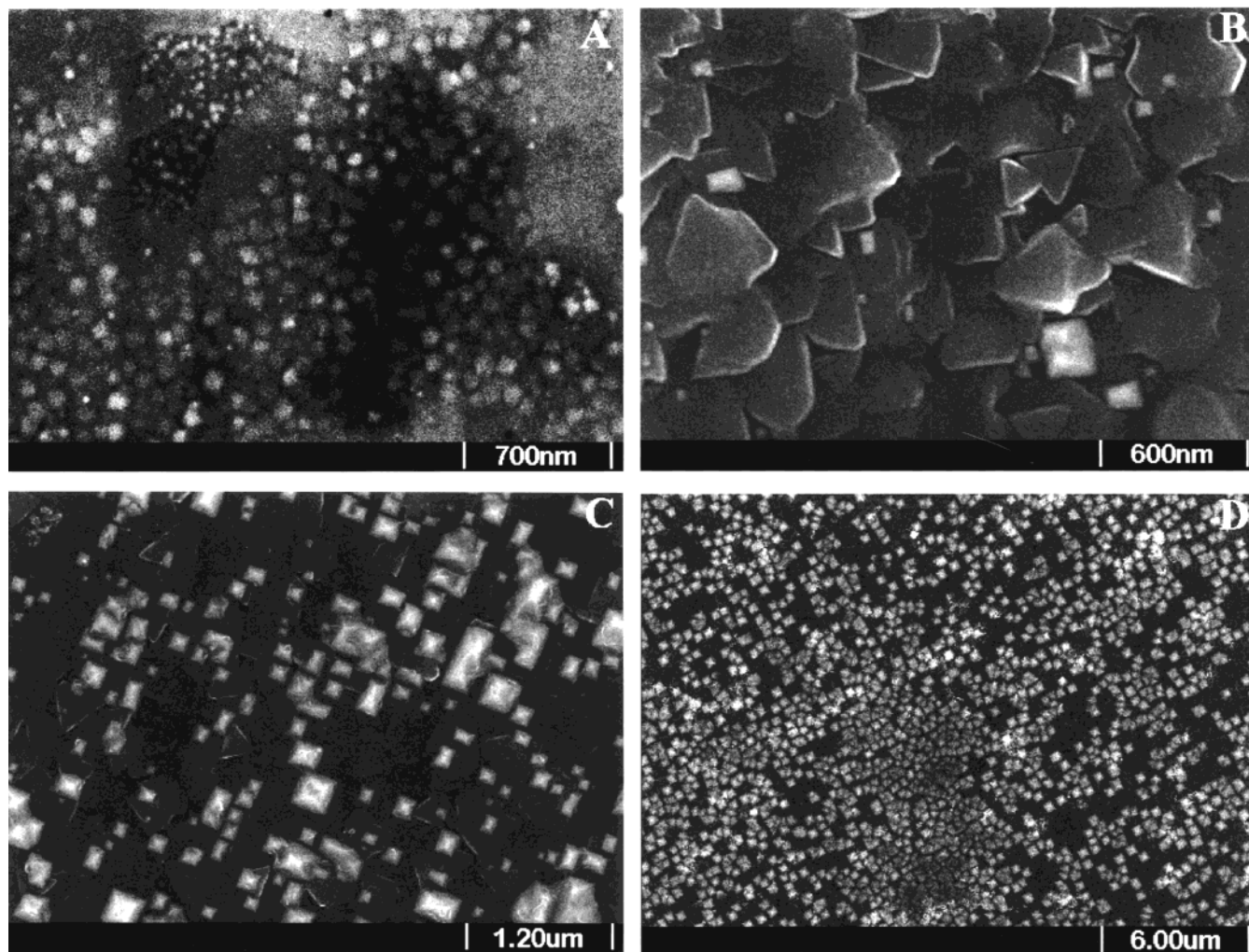


Figure 9. SEM images of Cu_2O films deposited on $\text{Cu}(100)$ grown to thicknesses of (A) 0.2, (B) 0.4, (C) 0.7, and (D) 2.6 μm . The transformation from growth in the [111] direction to the [100] can be visualized by the change from a film dominated by triangular facets to those of squares. Throughout the transformation, the facets remain oriented within the plane of the film surface.

values of $\chi^1 = 30.1^\circ$ and $\chi^2 = 38.6^\circ$. This tilting of the (111) planes by this amount is equivalent to saying that growth is now occurring in the [554] direction, resulting in a near-[111] orientated film.

The significance of the tilting of the (111) planes, or the corresponding growth along high-Miller index directions, as it relates to the nucleation of (100)-oriented crystals is not yet understood. The driving force for the transformation may be the relief of strain due to lattice mismatch. It is known that the atomic structures of high Miller index surfaces can be described in terms of terraces and steps.²⁴ This is much like Wild's observation that the tilting of the growth axis in the diamond films away from the [100] direction resulted in a roughened surface, with steps between adjacent (100) facets.²² In our system, it is possible that the development of steps may provide the nucleation sites for (100)-orientated growth. It is well-known that epitaxial growth of GaAs on Si single-crystal substrates often requires the miscutting of the Si crystal to create steps that serve as nucleation sites for the initial GaAs layer.²⁵

To visualize the transformation occurring in these films, SEM images were taken of the Cu_2O films at different stages of growth and are shown in Figure 9. The SEM image of a 0.2 μm film (Figure 9A) reveals crystals of indistinguishable shape, with diameter, D , ranging from approximately 65 to 90 nm. The image of a 0.4 μm film (Figure 9B) shows a combination of triangular and rectangular crystals, with $D_{\text{tri}} = 150\text{--}390$ nm and $D_{\text{rect}} = 40\text{--}150$ nm. The number of visible rectangles is very small compared to that of the triangles, agreeing with previous results that the film is primarily [111]-oriented. At a thickness of 0.7 μm (Figure 9C), the rectangular crystals have increased in size and number, corresponding to the increased growth in the [100] direction. The shape has also changed from rectangular to square. The visible triangles have also increased in size, but by a much smaller percent. Average crystal sizes are $D_{\text{tri}} = 260\text{--}480$ nm and $D_{\text{sqr}} = 90\text{--}240$ nm. The images agree with 2θ and pole figure X-ray data indicating that these thicknesses are transformation regions during which primary growth is changing from the [111] to the [100] direction. As can be seen in Figure 9D, at a film thickness of 2.6 μm , only squares are visible. Once again, this agrees well with the earlier XRD results, which indicated that the thicker film is predominantly [100]-oriented. The crystals visible

(24) Somorjai, G. A. *Introduction to Surface Chemistry and Catalysis*; Wiley: New York, 1994.

(25) Fischer, R. J.; Chand, W. F.; Kopp, W. F.; Morkoc, H.; Erickson, L. P.; Youngman, P. *Appl. Phys. Lett.* **1985**, *47*, 397.

at this point appear to be much more uniform in both size and shape, with an average size on the order of 400 nm. It is important to note that these images reveal not only geometric facets, but that these facets are aligned in the same direction within the plane of the film, indicating that the films are truly epitaxial. It is not clear from the images whether the film begins growth in only the [111] direction, or is simply dominated by growth in that direction. It does appear, however, that as the [100] direction becomes more dominant, some crystals continue to grow in the [111] direction, as indicated by the increased size of the triangles from 0.4 to 0.7 μm . Evidence of any tilting of the (111) planes cannot be seen from these images, as no cross-sectional view was available. Cross-sectional transmission electron microscopy (TEM) may prove ideal in gaining clear insight into the mode of film growth.

Conclusions

Epitaxial films of Cu_2O were electrodeposited onto Cu(111), (110), and (100) single crystals by reduction of copper(II) lactate in alkaline solution. X-ray studies of films grown on Cu(111) and (110) indicated that Cu_2O films grew epitaxially, with orientations following that of the Cu substrates.

Surprising results of both X-ray and SEM studies of films grown on Cu(100) indicate that the Cu_2O film

grows primarily in the near-[111] direction up to a critical thickness (≈ 360 nm) after which the growth occurs in both the near-[111] and [100] direction. At some thickness above 0.7 μm , nearly all growth appears to be in the [100] direction. At a thickness of 2.6 μm , the Cu_2O film is predominantly [100]-oriented and is epitaxial with the Cu substrate. It is suggested that the higher rate of growth in the [100] direction combats what may be the initial energetic driving force for growth in the [111] direction, resulting in an ultimate change in film orientation. It is further suggested that this change manifests itself by nucleating growth in high index directions, resulting in a slight tilting of the (111) planes relative to the substrate. This tilting appears to increase to a maximum angle of approximately 5.5°. Further research will focus on obtaining a better understanding of the mechanism of this transformation.

Acknowledgment. This work was supported by the National Science Foundation (CHE-9816484, DMR-9704288, DMR-0071365, and DMR-0076338), the Foundation for Chemical Research, and the University of Missouri—Rolla OURE program.

CM000707K